Joint Conference of 1996 International Computer Symposium
December 19~21, Kaohsiung, Taiwan, R.O.C.

A Radar and Electromagnetic Wave Analysis and Visualization System

Ching-Chian Chen *Shyh-Keng Jeng Jyh-Ren Jeng Ming Ouhyoung

Communication and Multimedia Laboratory
Department of Computer Science and Information Engineering
National Taiwan University, Taipei, Taiwan, R.O.C.

*Department of Electrical Engineering
National Taiwan University, Taipei, Taiwan, R.O.C.

Abstract

Vector field visualization plays an important role in science and engineering. Its applications range from highly practical, such as the design of new airplane wings, to the highly theoretical, such as the study of electromagnetic waves. In the first part of the paper, we will visualize the radar rays intersected with target and show some results of the analysis. While building the radar system, we are also interested in low frequency electromagnetic waves. Therefore in the second part, a systematic approach for visualizing electromagnetic waves is proposed. Six important but complex electromagnetic waves are visualized as field lines. In our system, field lines are clearly and efficiently rendered, and field magnitudes are indicated by different colors. And propagation, if any, is visualized by animation, with the motion of lines along the propagation direction .

Keywords: Computer graphics, radar cross section, Doppler spectrum, vector field visualization, streamline visualization, electromagnetic waves, Runge-Kutta method

1. Introduction

To design a target (airplane) by analyzing and predicting the intensity of the reflected radar wave is an interesting topic in the radar field [13,14,15]. The scattered signal of the radar from the target is very useful in target detection and recognition, hence many researchers have investigated in this topic for years. The Radar Cross Section (RCS) Analysis System is developed to simulate and analyze the scattered signal of radar from a target according to known theorems in the radar research field.

Users can take advantage of our system to draw planar charts to observe lots of RCS and Doppler spectrum numerical data. Radar waves, in a sense similar to light rays in ray-tracing, may bounce onto the target many times. Hence, we replace radar waves with rays in this paper. Similar idea first came from S. W. Lee in [15]. We use the technique of the ray tracing [8] to simulate the intersections of radar rays to airplane. This helps the designers to understand the scattering mechanism, and so is easy to modify the airplane structure to fit the required scattering characteristics.

When we consider of electromagnetic waves, however, it's no longer correct to simulate the wave behavior by ray tracing because of their low frequency property. Instead, we must draw the vector field lines to show the their behavior. In many electromagnetic wave textbooks, almost all sketches of electric or magnetic field lines for electromagnetic waves are shown in 2D diagrams. For instance, a sketch of the electric or magnetic field lines for the wave named rectangular waveguide TM_{11} mode in the book "Field and Wave Electromagnetics"[1] is shown in Figure1. However,

some important 3D information is not easy to be noticed, when visualizing a 3D vector field in 2D diagram. To improve upon this, a continuous representation using 3D lines for electromagnetic waves is proposed, combining with some visualization techniques, so that the features of the electromagnetic waves could be clearly and efficiently visualized.

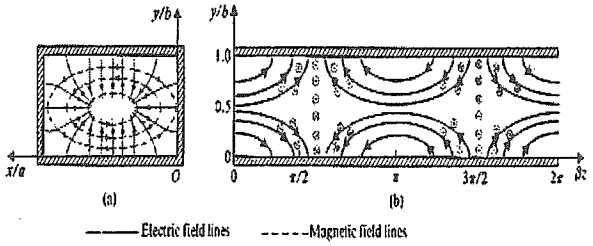

Figure 1. 2D diagram of electric and magnetic lines in textbook "Field and Wave Electromagnetics"

The research of vector fields visualization focuses on the representation of directional and multivariate data sets. Algorithms that can show such directional information have wide application across scientific domains. There are some commercial packages with the abilities to handle electromagnetic waves, which display as arrow lines with the length of the lines proportional to the vector magnitude. Arrow lines work well for 2D vector fields and even for 3D vector field if slices are taken through the field. Yet, they may cause visual clutter when the entire volume is large and complex. In recent years, other approaches were presented. These include sampling the vector field, such as streamlines [9,12], particle traces [11], and flow volume[6]. Another approach is to generate texture via a vector field, for example, spot noise [7] and line integral convolution [3,10]. These methods cover a variety of applications[5]. However most of them aim to visualize common stream lines, such as fluid dynamics, which are much different from electromagnetic waves. For example, we may observe a turbine stiring water; but we want to observe the propagation of electromagnetic waves, not their field direction. Furthermore, there are many rendered image sets in fluid-dynamics textbooks, but almost none for electromagnetic waves. These above facts indicate that too few systems are developed specifically for electromagnetic waves. Therefore it encourages us to devote to the visualization of electromagnetic waves.

The remainder of this paper is organized as follows. Section 2 describes the analysis and visualization of Radar waves. Section 3 explains the analysis of electromagnetic waves using vector field expressions. We use fourth order Runge-Kutta method in section 4 to solve this expression, and make some modification to achieve predetermined accuracy with minimum computational effort. Some specific visualization considerations for electromagnetic waves are proposed in section 5.

2. Radar wave analysis and visualization

First we render the target of the facet data which users designed. Users can change viewing angle through direct control or by specific value input to understand the geometry of the target.

The ray-shooting visualizer uses the technique of the ray tracing, and display the geometry of ray-target interaction. Users can change view angles to observe the ray-target interaction in arbitrary direction. Besides, user can specify the ray incident angle. When users set up the desired ray incident angle and launch the rays, the ray-shooting interaction can be visualized on the screen.We also allow users to view the rays with specific number of bounces. For instance, a user may be interested in the rays with 2 and 4 bounces, he or she can select the bounce number '2' and '4'. Therefore only those rays with 2 and 4 bounces can display on the screen. This provides users an ability to understand which components of the target contribute to these rays. (Figure 2)

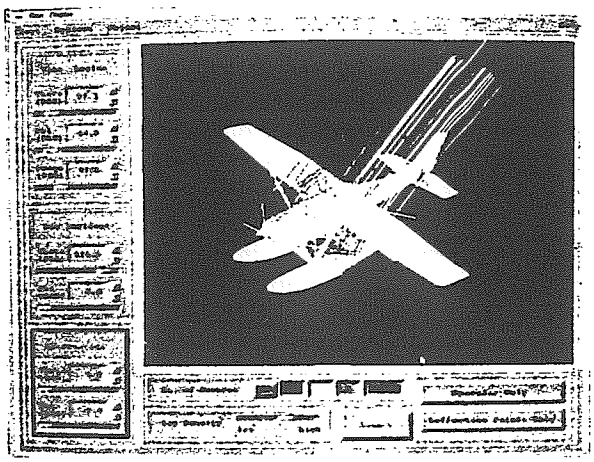

Figure 2. The radar to airplane intersection with hit ray bounce number represented as different colors

The Radar Cross Section (RCS) analysis is developed to simulate and analyze the scattered signal of radar from a target according to known theorems in the radar research field. The known theorems include the physical theory of diffraction (PTD), the physical optics approximation (PO), and the method of shooting and bouncing rays (SBR)[13]. The system plots the result of the Radar Cross Section computation in XY-plot representation, and users can analyze the scattering mechanism of the target. We take a simple rectangular plate as the target, and draw the diagram according the RCS computation results. (Figure 3)

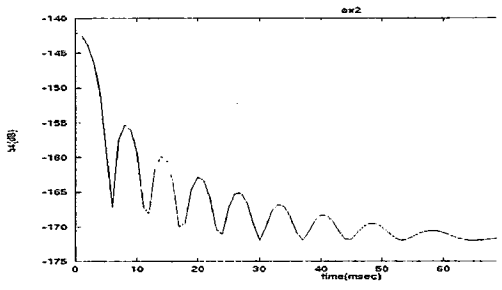

Figure 3. The plot of Radar Cross Section

In addition, we also compute Doppler Spectrum, which is caused by the rotating propeller hitting by radar waves (Figure 4). The density distribution of reflection changes as the differences of planes, and can be plotted as 2D figures wiht some signals transformation techniques to help recognizing the airplane.

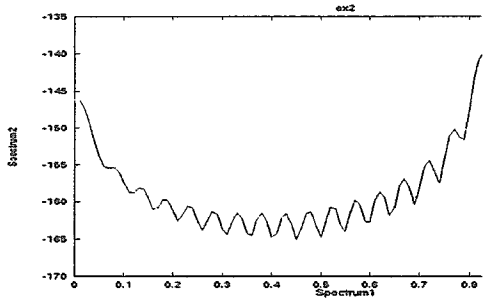

Figure 4. Computation of the Doppler Spectrum

The previous system [4] implementations just treat radar transmitter as infinite far away from the target, and the incident rays are parallel beams. But in practical condition, we must make some modification to perform near-field dynamic analysis, which radar antenna is put near a moving target, so as to meet to the real case.

3. Analysis of Electromagnetic Waves Field Expressions

We are also interested in general electromagnetic waves. Electromagnetic waves are vector fields. We consider a vector field defined by a map $v:R^3 \rightarrow R^3$, $x \rightarrow v(x)$, where x is a three-dimensional point (x, y, z) in the 3D volume. For example, for the rectangle waveguide TM_{11} mode in a rectangular cross section of widths a and b, the electric field component at a 3D point(x, y, z) is

$v(x, y, z) = (E_x(x, y, z), E_y(x, y, z), E_z(x, y, z))$, where

$$E_x(x,y,z)=\frac{\beta}{h^2}(\frac{\pi}{a})\cos(\frac{\pi}{a}x)\sin(\frac{\pi}{b}y)\sin(\omega*t-\beta*z),$$

$$E_y(x,y,z)=\frac{\beta}{h^2}(\frac{\pi}{b})\sin(\frac{\pi}{a}x)\cos(\frac{\pi}{b}y)\sin(\omega*t-\beta*z),$$

$$E_x(x, y, z)=\sin(\frac{\pi}{a}x)\sin(\frac{\pi}{b}y)\cos(\omega*t-\beta*z)$$

The directional structure of v can be graphically depicted by its integral curve lines, also called streamlines or field-lines. The streamline of the vector field has the property that its tangent vector at any point coincides with the direction of the field at that point. Considering a streamline P (Figure 5a), the vector at point (x, y, z) is (Ex, Ey, Ez). Streamline P could be treated as a curve composed of many segment (Figure 5b)). one segment *ds* is from (x, y, z) to (x+dx, y+dy, z+dz) (Figure 6), where dx, dy, dz are the projected length of ds on axis x, y ,z. And angle between ds and x, y, z is α_x, α_y, α_z respectively. The vector field at point (x, y, z) is (Ex, Ey, Ez), and the angles between vector (Ex, Ey, Ez) and x, y, z axis are β_x, β_y, β_z (Figure 7)

Since the streamline P is a curve with its tangent vector at any point coincides with the direction of the field at that point, we conclude that $\alpha_x = \beta_x$, $\alpha_y = \beta_y$, $\alpha_z = \beta_z$ Therefore

$\cos(\alpha_x)=\cos(\beta_x)$ ⇨ $dx/ds=E_x$ /norm

$\cos(\alpha_y)=\cos(\beta_y)$ ⇨ $dy/ds=E_y$ /norm (Eq.1)

$\cos(\alpha_z)=\cos(\beta_z)$ ⇨ $dz/ds=E_z$ /norm

$$norm = \sqrt{Ex * Ex + Ey * Ey + Ez * Ez}$$

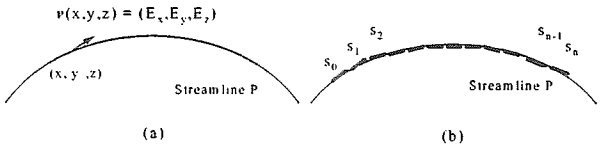

Figure 5. a streamline

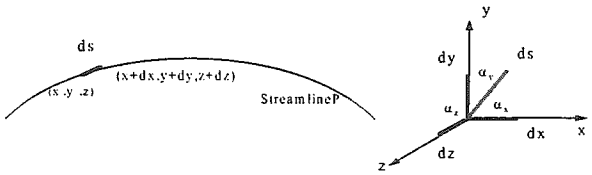

Figure 6. streamline analysis

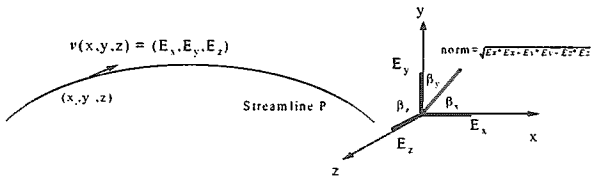

Figure 7. vector at point(x,y,z)

To find a streamline through point(x_0, y_0, z_0) the ordinary differential equation Eq.1 has to be solved, with an initial value(x_0, y_0, z_0). The initial point(x_0, y_0, z_0) is a random point located at the bounding box specified by the user. After integrating the three ordinary differential equations, we could construct a 3D streamline(also a field line).

4. Streamline Integration

To integrate Eq1, one approach is to try to determine the solution in a form from which we can compute exact numerical values. However, this approach doesn't always work, since the ordinary differential equations discussed in section 3 are too complicate. Another approach is to develop schemes for approximating numerical values of solutions to prescribed degree of accuracy. We have employed traditional fourth-order Runge-Kutta method (a fast and accurate general purpose streamline's integrator)[2].

From Eq1, we define a map f: $R^3 \rightarrow R^3$, $x \rightarrow f(x)$, where x is a 3D point. Let $f(x,y,z)=(E_x$ /norm, E_y /norm, E_z /norm). The fourth-order Runge-Kutta method requires 4 evaluations of the right hand side to proceed from some point x to some other point x_h located a stepsize h away on the same streamline, i.e.

$$k_1 = h f(x)$$

$$k_2 = h f(x+0.5k_1)$$

$$k_3 = h f(x+0.5\,k_2)$$

$$k_4 = h f(x+k_3)$$

$$\Delta x = k_1/6 + k_2/3 + k_3/3 + k_4/6$$

$$x_h = x + \Delta x + O(h^5)$$

The equation is called fourth-order because it approximates the solution with an error less than the power of h^4. As the Runge-Kutta method treats every step in a sequence of steps in identical manner, one must be careful of choosing the stepsize h. If h is too big, we save computational time, but lose accuracy. If h is too small, we achieve accuracy in these ordinary differential equations solutions with more computational effort.

In order to achieve some predetermined accuracy in these ordinary differential equations solution with minimum computational effort, we combine the Runge-Kutta method with an adaptive stepsize algorithm[2]. Implementation of adaptive stepsize control for Runge-Kutta method requires that the stepping signal truncation error information. With fourth-order Runge-Kutta method, the most straightforward technique is to doubling step[2]. We will take each step twice, once as a full stepsize h, then, independently, as two half stepsize h/2. Let us denote the exact solution from some point x to other point located a stepsize ahead on the same streamline by x' and the two approximate solution by x_h(one step h) and x_h· (two steps each of size h/2). Because the basic method is fourth-order, the exact solution and the two approximate solution are related by

$x' = x_h + c*h^5+O(h^6)+.....$

$x' = x_{h'}+ 2*c*(h/2)^5+O(h^6)+.....$

Let $\Delta = x_{h'} - x_h = (15/16)*h^5$, we can obtain the difference between the two numerical estimates. The value Δ is a convenient indicator of truncation error. The idea of adaptive stepsize is to choose h as large as possible while achieve a user defined error tolerance Δ. Since Δ scales as h^5, if a stepsize h results in error Δ, an optimized stepsize h' can be obtained by

$$h'=h*\sqrt[5]{\frac{\Delta_0}{\Delta}}$$

The equation is used in two ways: If Δ is larger than Δ_0, we repeat the current step with h=h'. If Δ is smaller than Δ_0, on the other hand, we proceed and take $h=\min(h',h_{max})$ for next iteration, where h_{max} is the maximum allowed stepsize. Obviously, the calculation of error information Δ will add to the computational overhead, but the investment will generally be repaid handsomely.

We apply fourth-order Runge-Kutta method and adaptive stepsize Runge-Kutta method to solve the rectangle waveguide TM_{11} mode field expression respectively, and compare their computational time and memory space utilization.

The rectangle waveguide TM_{11} mode propagates in a rectangular cross section of widths a and b. If a or b is larger, the field lines (electric and magnetic lines) in the rectangular cross section are longer. The average computational time for constructing 200 field lines(100 electric lines and 100 magnetic lines) and average memory space utilization for each line are given in Table 1. We find that when a>=2.0 and b>=2.0, time and memory utilization are both saved. It's easy to explain the result: Using the adaptive stepsize Runge-Kutta method, as a field line stretches longer(a or b becomes larger), a few smaller steps tiptoe through the region of high streamline curvature, while many great strides speed through smooth part of the field line.

	Adaptive stepsize Runge-Kutta	Fourth order Runge-Kutta
a=1.0, b=1.0	11	8
a=2.0, b=2.0	13	16
a=3.0, b=3.0	14	24
a=4.0, b=4.0	16	31
a=5.0, b=5.0	17	39

Table 1. Computational time(seconds). where a and b are the width and height of a rectangular waveguide

5. Implementation of Electromagnetic Wave Visualization

In this section, we discuss some characteristic of electromagnetic waves, that needed to taken into account when developing the electromagnetic waves visualization system.

5.1 System configuration

Our system is developed on an SGI Indigo graphics workstation in C language with Motif and OpenGL. Current version visualizes six electromagnetic waves. The six electromagnetic waves are rectangle waveguide TEmn and TMmm modes, electric dipole(near field and far field), and circular waveguide TEmn and TEmn modes. Users can adjust the parameters of these electromagnetic waves through graphical user interfaces. The field expressions of these six electromagnetic waves are so complex that the field lines of these waves could not be solved completely and so cannot clearly visualized by the famous mathematics software "Mathematica".

5.2 Vector Field Directions

Because the vector field directions coincide with the tangent vector of streamline, we can visualize the vector field directions by injecting one tracer particle into each streamline. When a tracer particle are injected to a streamline(for instance, inject an antielectron to a electric field line), it will trace the streamline

continuously to show the directions of vector field.

5.3 Plane Cutting

Sometimes 2D slices of 3D vector fields offers more meaningful information than 3D streamlines. For example, Figure 8 shows the 3D electric field lines of an electric dipole. Figure 9 shows the 2D electric field lines at plane x=0.0. We can see that the 2D slices of the electric field lines irradiated by a dipole show the wave pattern more clearly than that of the 3D one. We use the OpenGL command—plane clipping to complete the work. If we want to cut a 3D volume at plane Ax+By+Cz+D=0.0, we first reject the points on the half-space defined by a clipping plane Ax+By+Cz+D+d>0.0(d is a small value), then reject the points on the other half-space defined by a cutting plane Ax+By+Cz+D<0.0.

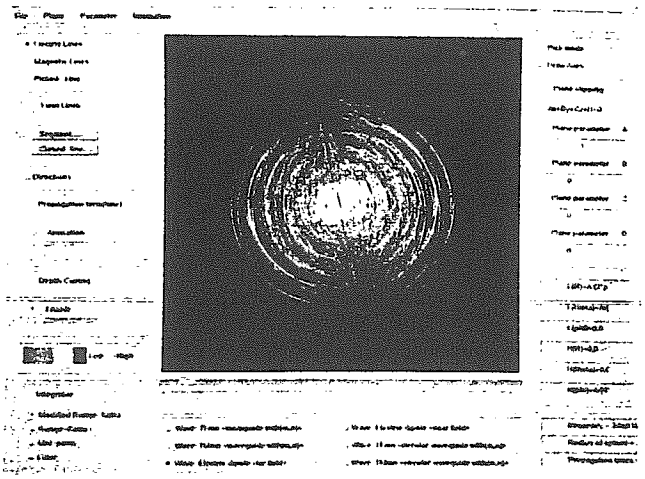

Figure 8. The 3D electric field lines of an electric dipole(far field)

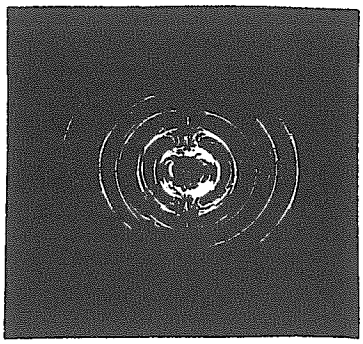

Figure 9. The 2D electric field lines at plane x=0.0(far field)

5.4 Depth Cueing

A depth-cueing algorithm provides the way to simulate the atmospheric attenuation from the model to the viewer. Figure 10 shows the effect of depth-cueing.

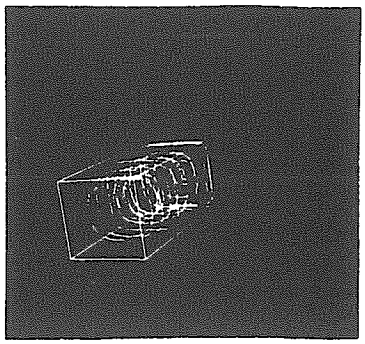

Figure 10. The effect of depth-cueing.

5.5 Pick a field line

Sometimes user want to focus on a specific streamline to see the behavior of the line. Our system offer a selection function to let user pick any streamline in the 3D volume.

5.6 Other Considerations

The magnitude of electromagnetic waves is indicated by color to clearly visualize the magnitude scattered over the whole 3D volume. If the electromagnetic waves will propagate with time, the transmission of waves is visualized by animation. Since some parameters are involved in the electromagnetic waves field expressions, user can adjust the parameters through a user–friendly interface to inspect the change of waves.

5.7 Results

Some of the results are shown is the following: Figure 11 and Figure 12 are the electromagnetic-wave named rectangle-waveguide TM_{11} modes, which was drawn in the form of streamlines. Figure 13 is the electric field lines of an electric-dipole Field expression of this wave is described in spherical coordinate. Figure 14 is circular-waveguide TM_{11} mode, which propagates inside round pipes. The field expression of this wave is described in cylindrical coordinate and a special function—Bessel function is involved in its field expressions.

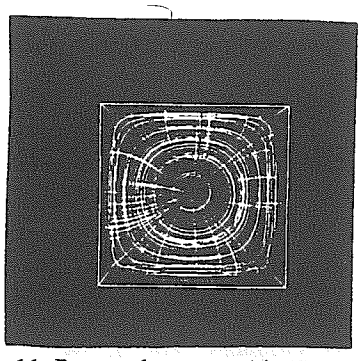

Figure 11. Rectangle-waveguide TM_{11} modes

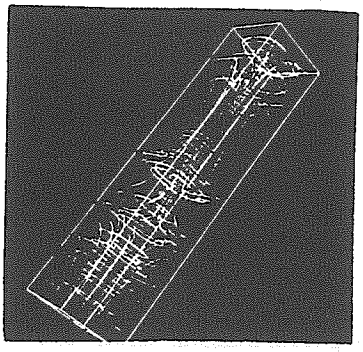

Figure 12. Rectangle-waveguide TM_{11} modes(another view)

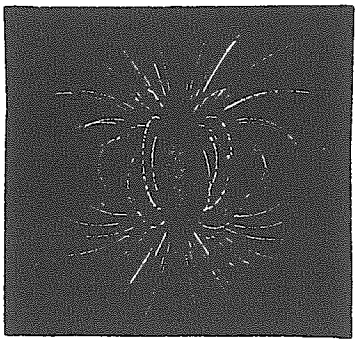

Figure 13. The electric field lines of electric-dipole(near field)

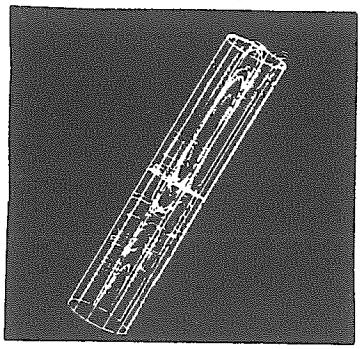

Figure 14. Circular-waveguide TM_{11} mode

6. Conclusions and Future directions

In this paper we analyzed two kinds of waves, including radar and electromagnetic waves. First, we implement the radar visualization system to help the design of airplanes. In particular the Radar Cross Section and Doppler Spectrum carry important information for designers. We will also extend our system to another kind of target – battleships, which incur more difficulities since the ocean itself is partially radio reflective.

We have proposed a streamline model for visualizing electromagnetic waves and present an electromagnetic wave analysis and visualization system that incorporated six types of electromagnetic waves. Combining with some visualization techniques, the features of electromagnetic waves could be clearly and efficiently visualized. The system is useful for better understanding of the Electromagnetic. In fact, one author, Shyh-Keng Jeng, used these rendered images and a sample aimation video to illustrate these complex waves in his electromagnetic course. The response from the students is both positive and highly encouraging.

7. Acknowledgments

The part of Near-Field Scattering Spectrum in this paper is supported by National Science Council under CS85-0210-D002-0012.

References

[1] David K. Cheng. "Field and Wave Electromagnetics"(second edition). Addison Wesley Press.

[2] William H.Press, Saul A. Teukolsky, William T. Vettering, and Brian P.Flannery. "Numerical Recipes in C: The Art of Scientific Computing." Cambridge University Press, Cambridge, 2nd edition, 1992.

[3] Detlev Stalling and Hans-Christian Hege. "Fast and resolution independent line integral convolution." *Proc. of SIGGRAPH'95. In Computer Graphics 29, Annual Conference Series, 1995, ACM SIGGRAPH, pp.249-256*

[4] Ching-Chian Chen, Ya Cheng, and Ming Ouhyoung. "Radar cross section analysis and visualization

system" 1995 *Computer Graphics Workshop, Taipei, Taiwan, pp.12-15 November 1995.*

[5] Richard, S. Gallagher, "Computer Visualization: Graphics Techniques for Scientific and Engineering Analysis", CRC Press ,1995.

[6] Nelson Max, Barry Becker, Roger Crawfis. "Flow volumes for interactive vector field visualization." *In Proc.of Visualization '93, pp. 19–24, IEEE Computer Society, 1993.*

[7] Jarke J. van Wijk. "Spot noise-texture synthesis for data visualization." Proc. of SIGGRAPH'91. In Computer Graphics, 25, pp. 309-318, 1991.

[8] Glassner, Andrew S. "Space Subdivision for Fast Ray Tracing." *IEEE CG&A, October 1984, p. 15-22.*

[9] Andrew J. Hanson, Hui Ma. "Quaternion Frame Approach to Streamline visualization". *IEEE Transaction on Visualization and Computer Graphics, Vol. 1, NO. 2, June 1995, pp.164-174*

[10] Lisa K. Forssell and Scott D. Cohen, "Using Line Integral Convolution for Flow Visualization: Curvilinear Grids, Variable-Speed Animation, and Unsteady Flows". *IEEE Transaction on Visualization and Computer Graphics, Vol. 1, NO. 2, June 1995, pp.133-141*

[11] David N. Kenwright and David A. Lane, "Interaction Time-Dependent Particle Tracing Using Tetrahedral Decomposition". *IEEE Transaction on Visualization and Computer Graphics, Vol. 2, NO. 2, June 1995, pp.120-129*

[12] Shyh-Kuang Ueng, Christopher Sikorski, and Kwan-Liu Ma, "Efficient Streamline, Streamribbon and Streamtube Constructions on Unstructured Grids", *IEEE Transaction on Visualization and Computer Graphics, Vol. 2, NO. 2, June 1995, pp.100-110*

[13] Ling, R. -C Chou, and S. W. Lee, "Shooting and bouncing rays: calculation the RCS of an arbitrarily shaped cavity", *IEEE Trans. Antennas Propagat., vol. AP-37, no. 2, pp. 194-205, February 1989.*

[14] Fuchs, Z. M. Kedem, and B. F. Naylor, "On visible surface generation by a priori tree structures", *ACM SIGGRAPH 80, Computer Graphics, vol. 14, no. 4, pp. 124-133, 1980.*

[15] Baldauf, S. W. Lee, L. Lin, S. K. Jeng, S. M. Scarborough, and C. L. Yu, "High frequency scattering from trihedral corner reflectors and other benchmark targets: SBR versus experiment", *IEEE Trans. Antennas Propagat., vol. AP-39, no. 9, pp. 1345-1351, September 1991.*